PCCP

Accepted Manuscript

ROYAL SOCIETY OF CHEMISTRY

www.rsc.org/pccp

Journal Name

ARTICLE

Fluorescent Emissions of Imide Compounds and End-Capped Polyimides Enhanced by Intramolecular Double Hydrogen Bonds

Received 00th January 20xx,
Accepted 00th January 20xx

DOI: 10.1039/x0xx00000x

www.rsc.org/

Kenta Kanosue and Shinji Ando*

The structure and optical properties of a newly synthesized imide compound (DHNHPI) that forms intramolecular double hydrogen bonds (*intra*-HBs) were investigated. This compound exhibits intense absorption at 372 nm (ε = 5,091 $cm^{-1}M^{-1}$) and strong emission at 427 nm (Φ = 0.507) in $CHCl_3$. Under basic conditions, the absorption and fluorescence peaks showed large bathochromic shifts by 70 nm and 95 nm, respectively, compared with the neutral condition due to conversion to anion form. Based on the single-crystal X-ray diffraction analysis, DHNHPI can exert intermolecular π–π interactions between adjacent molecules along the stacking direction, with resultant emission peaks exhibiting longer wavelengths (~525 nm) in the solid state. Moreover, an end-capped polyimide having DHNHPI moieties at the termini exhibited a strong fluorescence peak at 427 nm by photo-excitation at 332 nm. The large Stokes shift of 6,701 cm^{-1} clearly indicates the occurrence of an effective Förster-resonance energy transfer from the main chains to the fluorescent end-groups. These facts demonstrate that the incorporation of two –OH groups, which form *intra*-HBs, endows imide compounds and polyimides with enhanced fluorescence properties as well as high sensitivity to pH.

1. Introduction

Conjugated polymers such as poly(*p*-phenylene) and polyalkylthiophene exhibit distinct fluorescence properties associated with their conjugated π-orbitals that are delocalized along the polymer backbones. They have been expected to have applications in the fields of organic light-emitting diodes and plasma displays.[1,2] However, the thermal stabilities of such conventional fluorescent polymers, which are represented by glass transition temperatures (T_g) and thermal degradation temperatures (T_d), are not high enough to enable device fabrication processes and long-term durability in electronic and photonic industries.[3,4] High thermal stability as well as mechanical, chemical, and environmental stabilities are strongly desired for fluorescent polymers used in modern optoelectronic and photonic applications.

Polyimides (PIs) are a class of representative high-performance polymers in which the repeating unit consists of alternating dianhydride and diamine moieties. They are known as super-engineering plastics with their outstanding thermal stabilities arising from their rigid chemical structures and strong interchain interactions; therefore, they are widely used in the aerospace, electric, micro-electronic, and photonic industries.[5] Recently, an attempt has been made to endow PIs with fluorescence properties as a novel optical functionality. Elaborate investigations of PI fluorescence properties have been performed because PIs are promising candidates for novel fluorescent materials whose properties are sustainable under high temperatures during device fabrication.[6-12]

Fluorescence properties of organic molecules are usually examined in diluted solutions, whereas most PIs are insoluble in organic solvents because of their rigid main-chain structures and strong interchain interactions. Therefore, the use of low-molecular-weight (low-Mw) imide model compounds soluble in polar solvents is helpful to understand and predict the fluorescence properties of PIs.[13-16] Recently, the present authors assigned the electronic transitions of imide compounds and PIs with the aid of time-dependent density functional theory (TD-DFT) calculations.[10] It has been known that wholly aromatic PIs undergo two types of electronic transitions after photo-irradiation by UV or short-wavelength visible light. The first type is a "locally excited" (LE) transition that occurs in the dianhydride moieties, and the second type is a "charge transfer" (CT) transition originating from the CT complexes formed between the electron-donating diamine and electron-accepting dianhydride moieties. Furthermore, the LE transitions can be classified into "π–π*" and "n–π*" transitions, and the LE(π–π*) transitions occur in π-conjugated components of the dianhydride moieties, whereas the LE(n–π*) transitions originate from the lone-pair electrons (n-orbital) located at the carbonyl oxygen and nitrogen atoms in the imide rings. In general, LE(π–π*)transitions of PIs have higher oscillator strengths (f), whereas those of LE(n–π*) transitions are very low. We have found that the

[a] Department of Chemistry & Materials Science, Tokyo Institute of Technology, Ookayama 2-12-1-E4-5, Meguro-ku, Tokyo 152-8552, Japan. E-mail: sando@polymer.titech.ac.jp

† Electronic Supplementary Information (ESI) available: [The calculated MOs of NHPI, 3HNHPI, and DHNHPI (TD-DFT method at the B3LYP/6-311++G(d,p) level); the absorption and fluorescence spectrum of DMNHPI in $CHCl_3$; the calculated electronic transitions of the anion form of DHNHPI ($DHNHPI^-$) in the optimized S_0 geometry; the spatial distributions of the HOMO and LUMO of $DHNHPI^-$ (TD-DFT method at the B3LYP/6-311++G(d,p) level); the ATR FT-IR spectra of PI films; the TGA curve of the PI films; the calculated energies (E(RB3LYP)) of DHNHPI isomers and tautomers in the optimized S_0 geometry; and the crystal data and experimental details of 3HNHPI and DHNHPI.]. See DOI: 10.1039/x0xx00000x

PIs whose lowest electronic transition ($S_0 \rightarrow S_1$) is an LE(π–π*) transition actually exhibit strong fluorescence.[10] For example, semi-aliphatic PIs synthesized from dianhydrides with large π-conjugation and alicyclic diamines without π-electrons show relatively high fluorescence quantum yields (Φ). This behavior is explainable by enhancement of the LE(π–π*) transition due to large π-conjugation and restraint of the CT transition with a very small f value due to a weak electron-donating alicyclic diamine structure. We synthesized a highly fluorescent PI film from 1,4-bis(3,4-dicarboxyphenoxy)benzene dianhydride and 4,4'-diaminocyclohexylmethane (DCHM), whose Φ value was 0.11.[10] This PI demonstrated very high thermal stability (with a resultant 5% weight loss) at a thermal decomposition temperature T_d^5 of 425 °C and a T_g of 259 °C, which are much higher than those of π-conjugated fluorescent polymers.[3,4]

Moreover, we found that the formation of intramolecular hydrogen bond (*intra*-HB) between –OH and C=O groups in imide compounds containing hydroxy-phthalimide moiety significantly stabilizes the lone-pair *n*-orbitals located at the oxygen of the imide C=O group. This effectively lowers the transition energy of the LE(π–π*) transition with respect to that of the LE(n–π*) transition, and thus the $S_0 \rightarrow S_1$ transition becomes an LE(π–π*) transition.[16,17] Additionally, an OH-containing imide model compound, 3-hydroxy-*N*-cyclohexylphthalimide (3HNHPI), which forms a stable *intra*-HB between the phenolic –OH and imide C=O group, exhibits a strong fluorescence with a very large Stokes shift (ν = 11,394 cm^{-1}) via an excited-state intramolecular proton transfer (ESIPT).[16] The ESIPT phenomena of low-Mw compounds have been widely studied in the solution state due to their interesting photophysical behaviors in the excited-state.[18-20] ESIPTs can be observed for molecules whose proton-donating moieties (e.g., –OH or –NH– groups) and proton-accepting moieties (e.g., >C=O or –N=) come spatially close by forming *intra*-HBs.

Furthermore, the excited-state intramolecular double proton transfer (ESIDPT) process, in which two protons separately involved in *intra*-HB are transferred by photo-irradiation, has also attracted interest due to its importance in chemistry and biology.[21-23] Among low-Mw compounds inspiring ESIDPT, the question of whether the two-proton transfer processes take place concertedly, or stepwise, has been discussed. For instance, Glasbeek et al.[24-28] have performed extensive studies regarding the ESIDPT mechanism in [2,2'-bipyridyl]-3,3'-diol ($BP(OH)_2$) using a fluorescence up-conversion technique and confirmed that $BP(OH)_2$ exerts a bifurcated type of ESIDPT that produces both a single-proton-transferred form (mono-keto form) and a double-proton-transferred form (di-keto form) nearly simultaneously (within a duration of ~100 fs).

The fluorescence properties of ESIPT compounds could be sensitive to environmental conditions (e.g., dielectric constant, temperature, pH, and pressure) because ESIPTs involve transferrable protons. In general, ESIPTs are frequently observed when dissolved in hydrocarbons or nonpolar solvents; thus, fluorescence from the excited keto form is predominately observed. On the other hand, when dissolved in polar or protic solvents, ESIPTs are partially inhibited by solvent molecules, and the fluorescence from the enol form is hence observable.[29-35] For example, a bright fluorescence is emitted from the keto form (500 nm) of 2-(2'-hydroxyphenyl)benzoxazole (HBO) via an ESIPT when excited at 320 nm in *n*-hexane, though a fluorescence peak from the enol form is observed at 365 nm in methanol in addition to the fluorescence from the keto form.[36] This behavior occurs because the –OH group of HBO forms intermolecular HBs with solvent methanol, which results in a partial inhibition of proton transfer. Fin et al.[37] investigated the fluorescence properties of an OH-inclusive naphthalene diimide under variable pH conditions. In an acidic environment (pH = 3), the compound exhibited dual fluorescence from its enol (500 nm) and keto forms (630 nm). On the other hand, in an alkaline (basic) environment (pH = 13), proton transfer was effectively inhibited by the deprotonation of –OH groups by the base. In this case, an anion form was generated, and only characteristic absorption and emission bands of the anion form were observed. As explained above, introduction of –OH groups and formation of *intra*-HBs cause significant changes in the fluorescence properties of imide compounds. Accordingly, by elucidating the influence of introduced –OH groups and the formation of *intra*-HBs, we can expect new and valuable design-concept knowledge for highly fluorescent PIs.

To thus investigate the effects of –OH groups on the fluorescence properties of imide compounds and PIs, firstly, an imide compound having two –OH groups in its anhydride moiety (DHNHPI: Fig. 1c) was synthesized, and then its fluorescence properties in the solution and solid state were extensively examined by comparing with those of *N*-cyclohexylphthalimide (NHPI: Fig. 1a) and 3HNHPI (Fig. 1b). Secondly, the fluorescence properties of DHNHPI under alkaline conditions were measured to investigate the responsivity of the fluorescence properties to such conditions. Additionally, an end-capped PI having DHNHPI moieties at the termini of the polymer chains of the fluorescent PI (PI-DHPA: Fig. 1f) was newly synthesized, and its optical absorption and fluorescence properties were examined in the solid-film state.

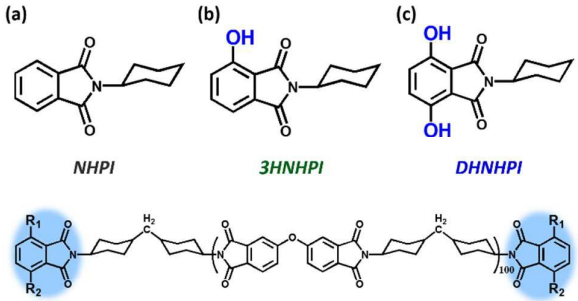

Fig. 1. Structures of Imide Compounds and End-capped PIs. (a) NHPI, (b) 3HNHPI, (c) DHNHPI, (d) PI-PA, (e) PI-3HPA, and (f) PI-DHPA.

2. Experimental

2.1. Materials[16]

3,6-Dihydroxyphthalonitrile (1), purchased from Tokyo Kasei Kogyo Co. Ltd., was decolorized by activated carbon twice and was recrystallized from a methanol/$CHCl_3$ mixed solution. Cyclohexylamine, purchased from Kanto Chemical Co. Inc., was purified by distillation under reduced pressure. An imidization promoter, 9,10-dihydro-9-oxa-10-phosphaphenanthrene-10-oxide (HCA), purchased from Tokyo Kasei Kogyo Co. Ltd., was used as received. 4,4'-Oxydiphthalic dianhydride (ODPA), supplied by Shanghai Institute of Synthetic Resins, was dried at 150 °C for 12 h under reduced pressure. 4,4'-Diaminocyclohexylmethane (DCHM), purchased from Tokyo Kasei Kogyo Co. Ltd., was purified by recrystallization from *n*-hexane and subsequent sublimation under reduced pressure. *N*,*O*-Bis(trimethylsilyl)trifluoroacetamide (BSTFA, ≥99%) and *N*,*N*-dimethylacetamide (DMAc, anhydrous), purchased from Aldrich Chemical Co., were used as received. $CHCl_3$ (fluorescence grade), purchased from Kanto Chemical Co. Inc., was used without further purification. 1,8-Diazabicyclo[5.4.0]undec-7-ene (DBU), purchased from Tokyo Kasei Kogyo Co. Ltd., was purified by distillation under reduced pressure.

2.2. Synthesis of Imide Compound

2.2.1. 3,6-Dihydroxyphthalic Acid (2)[38-40]

The synthetic scheme of DHNHPI is shown in Scheme 1. Compound 1 (8.0 g, 50 mmol) and potassium hydroxide (50.7 g, 904 mmol) were added to water (50 mL) and were refluxed for 3 h under nitrogen flow. After cooling to 0 °C, the mixture was acidified with 20% sulfuric acid and extracted with ethyl acetate (10 × 50 mL). The combined organic extracts were dried with magnesium sulfate, filtrated, and concentrated by rotary evaporator. The residual solution was precipitated with *n*-hexane, filtrated, and dried under vacuum, with a faint yellow powder ultimately being obtained (7.0 g, 35 mmol, yield 71%). ^{1}H NMR (400 MHz, DMSO-d_6, ppm): δ = 6.93 (s, 2H, Ph), 10.13 (s, 2H, OH). ^{13}C NMR (100 MHz, DMSO-d_6, ppm): δ = 117.13, 120.70, 149.63, 169.34.

2.2.2. 3,6-Dihydroxyphthalic Anhydride (DHPA: 3)[41,42]

Thionyl chloride (30 mL) was added dropwise to compound 2 (5.0 g, 25 mmol) over 15 min at 60 °C. The solution was heated to 90 °C and was refluxed for 12 h under nitrogen flow. The excess thionyl chloride was removed by distillation under reduced pressure, with a brown powder ultimately being obtained (4.8 g, 24 mmol, yield 97%). To purify DHPA for the synthesis of an end-capped PI, the crude product was recrystallized from an ethyl acetate/*n*-hexane mixed solution and was subsequently sublimed under reduced pressure, with a yellow powder ultimately being obtained. ^{1}H NMR (400 MHz, DMSO-d_6, ppm): δ = 7.23 (s, 2H, Ph), 10.13 (s, 2H, OH). ^{13}C NMR (100 MHz, DMSO-d_6, ppm): δ = 113.18, 127.31, 149.90, 161.26.

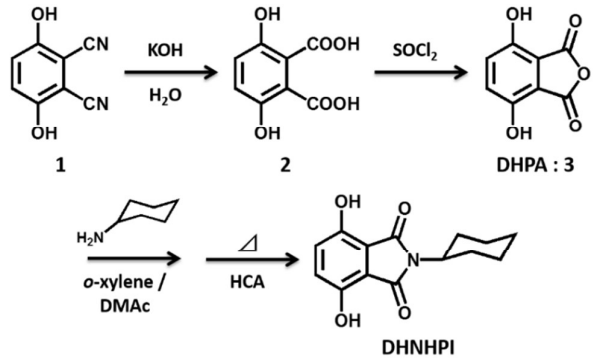

Scheme 1. Synthetic Scheme of DHNHPI.

2.2.3. 3,6-Dihydroxy-*N*-Cyclohexylphthalimide (DHNHPI)

Compound 3 (3.0 g, 17 mmol) was dissolved in *o*-xylene (10 mL)/DMAc (8 mL) mixed solution with cyclohexylamine (1.7 g, 17 mmol) added and was heated at 50 °C for 1 h under nitrogen flow. A catalytic amount of HCA was added to the reaction solution and refluxed with a Dean-stark apparatus at 150 °C for 3 h. After cooling to room temperature, the solution was poured to excess water, and the precipitate was filtrated and dried under vacuum. The crude product was purified by column-chromatography on silica gel ($CHCl_3$) and recrystallization from a $CHCl_3$/*n*-hexane mixed solution, with yellow crystals ultimately being obtained (3.2 g, 12 mmol, yield 72%). ^{1}H NMR (400 MHz, DMSO-d_6, ppm): δ = 1.06–1.36 (m, 3H, CH_2), 1.56–1.83 (m, 5H, CH_2), 1.99–2.21 (m, 2H, CH_2), 3.87 (m, 1H, N–CH), 7.04 (s, 2H, Ph), 10.12 (s, 2H, OH). ^{13}C NMR (100 MHz, DMSO-d_6, ppm): δ = 25.01, 25.62, 29.43, 49.30, 113.89, 125.73, 147.92, 166.38. Found: C, 64.62; H, 5.72; N, 5.28; O, 24.59 %. Calc. for $C_{14}H_{15}NO_4$: C, 64.37; H, 5.75; N, 5.36; O, 24.52 %. HRMS (EI) *m/z* $[M]^+$ Found: 261.1004. Calc. for $C_{14}H_{15}NO_4$: 261.1001.

2.3. Synthesis of End-Capped Polyimide (PI-DHPA)[16]

The synthetic scheme of PI-DHPA is shown in Scheme 2. The precursor of the ODPA/DCHM PI (polyamic acid silylester [PASE]) was prepared by the *in-situ* silylation method.[43,44] The molar ratio of the end group (*r*) for end-capped PIs is defined as follows:

$$r = \frac{100 \times m(\mathrm{end})}{m(\mathrm{end}) + 2m(\mathrm{DA})}$$

where *m*(end) and *m*(DA) are the molar quantities of the end group and dianhydride, respectively. In the present study, since anhydride of DHPA was used as an end group, PASEs having $-NH_2$ groups at the termini of the molecular chain were prepared. According to the above equation, the number-average degree of polymerization (*n*) of PASEs is given by (−1+200/*r*), and the value of *r* was set to 1.98, which corresponds to *n* = 100. The preparations of the PASE solution with *n* = 100 and a corresponding PI film are described below.

DCHM (1.0 g, 5 mmol) was dissolved in DMAc (13 mL) with BSTFA (1.2 g, 5 mmol) then slowly added, followed by stirring for 30 min. Trimethylsilylation of the diamine $-NH_2$ groups by BSTFA can avoid potential salt formation between unreacted $-NH_2$ and –COOH groups. ODPA (1.4 g, 5 mmol) was added to the solution and stirred at room temperature for 24 h. DHPA (34 mg, 0.2 mmol) was then added and was stirred at room temperature for 24 h. DHPA reacted with the terminal $-NH_2$ groups of the PASE chains, yielding a terminal-modified PASE. A viscous PASE solution was spin-coated

Journal Name

ARTICLE

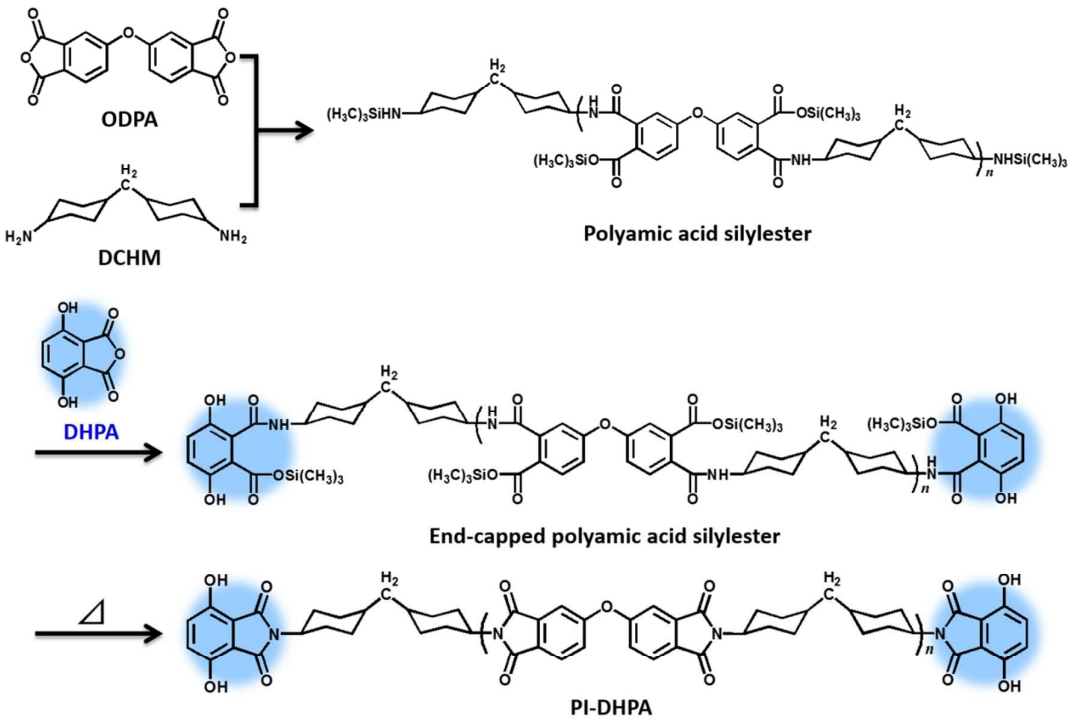

Scheme 2. Synthetic Scheme of PI-DHPA.

onto a fused silica substrate, followed by soft-baking at 70 °C for 1 h. Subsequent thermal imidization (by a one-step imidization procedure) was then enacted via a 4.6 °C/min increase in heating rate from 70 °C to 220 °C, with the final curing condition being set to 220 °C for 1.5 h. All curing procedures were conducted under nitrogen flow.

2.4. Measurements

2.4.1. UV-vis Absorption and Fluorescence Excitation/Emission Spectra

A series of $CHCl_3$ solutions of DHNHPI were prepared with varying concentrations in the range of 10^{-6} to 10^{-4} M. The UV-vis absorption and fluorescence spectra of the solutions and film samples were measured by a Hitachi U–3500 spectrophotometer and Hitachi F–4500 fluorescence spectrometer, each individually equipped with a photomultiplier tube (HAMAMATSU R3896 and R928, respectively). The fluorescence spectra of the solutions were measured without degassing, and the front-face method was adopted for the film samples to reduce self-absorption of the emitted fluorescence. The emission spectra were measured from the excitations at peak wavelengths (λ_{ex}) of the corresponding excitation spectra. In contrast, the excitation spectra were measured by monitoring the fluorescence intensities at peak wavelengths (λ_{em}) of the emission spectra. The measured spectra were not corrected for the sensitivity of photomultiplier tubes to fluorescence wavelengths. The fluorescence quantum yields (Φ) of the solution and film samples were alternatively measured by using a calibrated integrating sphere (HAMAMATSU C9920) connected to a multichannel analyzer (HAMAMATSU C7473), via an optical fiber link. In this measurement, the samples were excited at a controlled λ_{ex} using a monochromated xenon light source, and the solution samples were degassed by argon prior to measurements.

2.4.2. X-Ray Single-Crystal Structural Analysis

A single crystal of 3HNHPI was obtained by slow evaporation from acetonitrile, and that of DHNHPI was obtained by recrystallization from a $CHCl_3$/*n*-hexane mixed solution. The X-ray diffraction (XRD) data for the crystalline structural analyses were recorded on a Rigaku R-AXIS RAPID-II (Cu Kα). The structures were analyzed by direct methods and refined by the full-matrix least-squares method with SHELXS-97 software.[45] All non-hydrogen (non-H) atoms were refined with anisotropic temperature factors. The positions of hydrogen (H) atoms within –OH groups were calibrated from the

difference electron density maps. Other H atoms were inserted at standard positions and refined by a riding model.

2.4.3. Other Measurements

NMR spectra were measured with a JEOL AL-400 spectrometer operating at a ^{1}H resonance frequency of 400 MHz. The chemical shifts were reported in ppm (δ) using tetramethylsilane (TMS) as the standard. The Fourier-transform infrared (FT-IR) absorption spectra of imide compounds were measured by the KBr method in the range from 400 cm^{-1} to 4000 cm^{-1} using a Thermo-Nicolet Avatar-320 spectrometer. FT-IR spectra of PI films were measured in the range from 650 cm^{-1} to 4000 cm^{-1} using a Thermo-Fisher Avatar-320 spectrometer, equipped with a Thunderdome attenuated total reflection (ATR) attachment (with an incident angle of 45°). The prism (internal reflection element) was made of germanium crystal with a refractive index of 4.0. The thermogravimetric analyses (TGA) were conducted with a Shimadzu DTG-60 analyzer with a heating rate of 10 °C/min. The film thicknesses of the PI films were measured with a probe-pin-type surface profilometer (DEKTAK-III).

2.5. Quantum Chemical Calculation

TD-DFT was adopted to calculate the electronic structures and spectroscopic properties of the imide model compounds. The three-parameter Becke-style hybrid functional (B3LYP) was used, and the geometry optimizations with the 6-311G(d) basis-set were performed for the ground-state (S_0).[46-48] The 6-311++G(d,p) basis-set was used for generating molecular orbitals (MOs), and for calculating vertical one-electron excitation wavelengths and oscillator strengths (f) for the S_0 geometries. All calculations were performed with the Guassian-09 B.01 program package, which implements analytical gradients at the TD-DFT level.[49] This package is regularly available for utilization at the Global Scientific Information and Computing Center, Tokyo Institute of Technology.

3. Results & Discussion

3.1. Fluorescence Properties of DHNHPI

Characterization of Imide Compounds

Fig. 2a shows the FT-IR spectra of powder samples of NHPI, 3HNHPI, and DHNHPI measured by the KBr method. DHNHPI displays absorption peaks at 1660–1720 cm^{-1}, 2900 cm^{-1}, and 3400 cm^{-1}, which are assignable to the asymmetric stretching of C=O bonds (ν_{CO}) in the imide rings, the stretching of C–H bonds of the cyclohexyl rings, and the phenolic O–H stretching bands, respectively.[16] Fig. 2b shows the magnified ν_{CO} bands for which the peak intensities are normalized. Compared with the ν_{CO} peak of NHPI, those of 3HNHPI and DHNHPI are visibly shifted to lower wavenumbers by 22 cm^{-1} and 33 cm^{-1}, respectively, which is likely caused by the weakening of the C=O bonds due to formation of *intra*-HBs between the imide C=O and phenolic –OH groups in the latter compounds.[16,50,51] The ν_{CO} band of DHNHPI exhibiting a symmetric shape has a similar bandwidth to that of NHPI, which indicates that both DHNHPI phenolic –OH groups form *intra*-HBs with adjacent C=O groups.

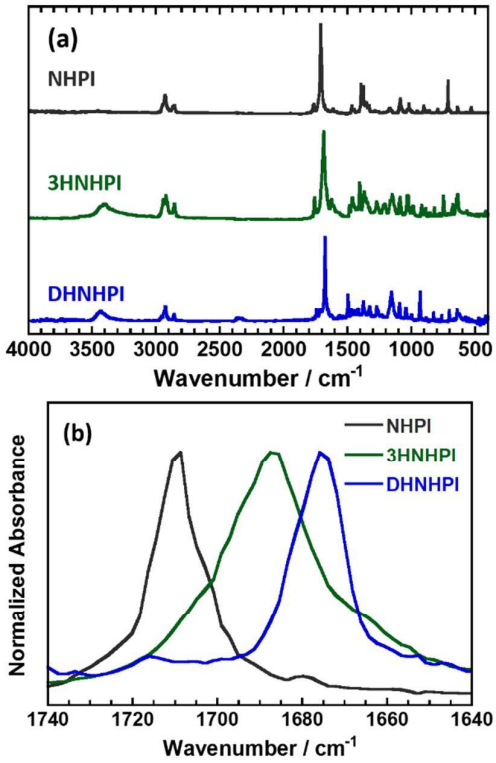

Fig. 2. FT-IR spectra of NHPI, 3HNHPI, and DHNHPI. Spectra are normalized at asymmetric C=O stretching bands. (a) Overall view and (b) enlarged view at near asymmetric C=O stretching bands.

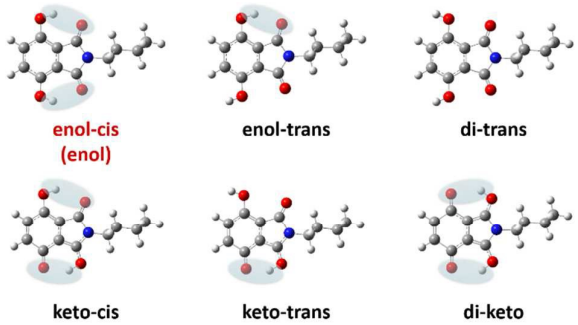

Fig. 3. Possible structures of isomers and tautomers of DHNHPI with different manners of *intra*-HBs.

DHNHPI is expected to have six kinds of isomeric and tautomeric structures with different modes of *intra*-HBs, as shown in Fig. 3. According to the DFT calculations, the most energetically stable structure in the ground state (S_0) is the enol-cis isomer. The results of geometry optimization at the S_0 state for all six structures are shown in Table S1 in the Supplementary Information. Assuming a Boltzmann distribution at room temperature, the proportions of the enol-cis isomer are estimated to be higher than 99.98%; thus, the existence of other isomers/tautomers is negligible. Hereafter, DHNHPI is assumed to exist as the enol-cis isomer (enol form) in the S_0 state, with both phenolic –OH groups forming *intra*-HBs, as evidenced by X-ray single-crystal structural analysis (see below).

Fluorescence Properties in $CHCl_3$ Solution

Fig. 4a and 4b show the UV-vis and fluorescent emission spectra of NHPI, 3HNHPI, and DHNHPI dissolved in $CHCl_3$ (5×10^{-5} M), respectively. Table 1 summarizes the absorption peak wavelengths (λ_{abs}), molar absorption coefficients (ε), excitation/emission wavelengths λ_{ex}, λ_{em}), Stokes shifts (ν), and fluorescence quantum yields (Φ) estimated for these compounds. Moreover, Table 2 lists the vertical excitation wavelengths, oscillator strengths (f), dominant contributing MOs, and assignments of electron transitions calculated for the imide compounds in the optimized S_0 geometry. The spatial distributions of the calculated MOs are illustrated in Fig. S1 in the Supplementary Information. We have reported that the $S_0 \rightarrow S_1$ transitions of NHPI and 3HNHPI are attributable to the LE(n–π*) and LE(π–π*) transition, respectively.[16] Note that the absorption peak of NHPI at 294 nm does not correspond to the $S_0 \rightarrow S_1$ transition, but rather to the $S_0 \rightarrow S_4$ transition. Since the absorption band corresponding to the $S_0 \rightarrow S_1$ transition is very weak, this band is faintly observed as a weak tailing at about 320 nm. In the emission spectrum of NHPI excited at 295 nm, a very weak fluorescence peak (Φ = 0.007) is observed, which originates from the small f value of the LE(n–π*) transition corresponding to the $S_0 \rightarrow S_1$ transition. On the other hand, the LE(π–π*) absorption of 3HNHPI observed at 328 nm is relatively intense because the $S_0 \rightarrow S_1$ transition is the allowed LE(π–π*) transition, which has a large f value of 0.093. In the emission spectrum of 3HNHPI excited at 332 nm, a strong fluorescence peak at 534 nm (Φ = 0.352) with a very large Stokes shift (ν = 11,394 cm^{-1}) is observed, which is attributable to the excited keto form generated via ESIPT. According to the TD-DFT calculation for the keto form of 3HNHPI, the f value for the $S_0 \rightarrow S_1$ transition is very large (f = 0.1438), which supports the enhanced fluorescent emission scenario.

In the UV-vis spectrum of DHNHPI, an intense absorption peak is observed at 372 nm in Fig. 4a. Compared with the peaks of NHPI and 3HNHPI, this peak appears at a much longer wavelength by 44–78 nm. The calculated transition of DHNHPI appearing at 363.7 nm ($S_0 \rightarrow S_1$) with a large f value (0.1498) is assignable to an LE(π–π*) transition (see Table 2); thus, the intense absorption is readily attributable to this band. The same kind of absorption peaks corresponding to allowed LE(π–π*) transitions of the three imide compounds are shifted to longer wavelengths on the order of NHPI (294 nm) < 3HNHPI (328 nm) < DHNHPI (372 nm). The bathochromic shifts should be mainly caused by delocalization of π-electrons associated with the formation of *intra*-HBs.[52] DFT calculation indicated that the n-orbitals of 3HNHPI and DHNHPI are energetically stabilized by the formation of *intra*-HBs. In particular, the formation of double *intra*-HBs having a symmetrical structure in DHNHPI expands its π-conjugation at the phthalic imide moiety, and it significantly enhances the probability of π–π* transitions with increasing the ε and Φ values compared with 3HNHPI. In the emission spectrum of DHNHPI excited at 369 nm, an intense fluorescence peak is observed at 427 nm with a high Φ value of 0.507. However, the Stokes shift (ν = 3,463 cm^{-1}) is much smaller than that of 3HNHPI (ν = 11,394 cm^{-1}). Since the Stokes shift is sensitive to the changes in the geometric and electronic structures between the ground- and excited-states, the structural changes caused by the excitation of DHNHPI are supposed to be small. Moreover, the spectral shape of the fluorescent emission is a mirror image of the absorption spectrum. These facts distinctly indicate that fluorescence is emitted from the enol form (in the excited-state) without undergoing an ESIPT in $CHCl_3$.

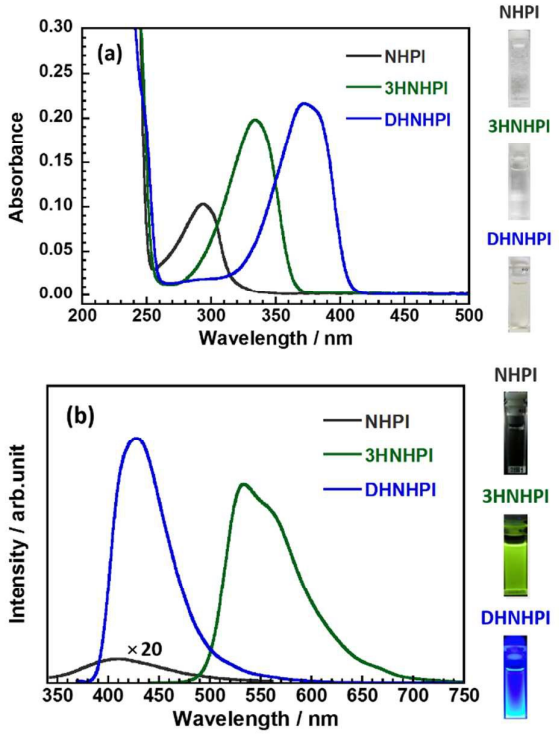

Fig. 4. (a) UV-vis and (b) emission spectra of NHPI, 3HNHPI, and DHNHPI (5×10^{-5} M) in $CHCl_3$. Excitation wavelengths are 295 nm (NHPI), 332 nm (3HNHPI), and 369 nm (DHNHPI).

Table 1. Experimental Absorption Wavelengths (λ_{abs}), Molar Absorption Coefficients (ε), Excitation/Emission Wavelengths (λ_{ex}, λ_{em}), Stokes Shifts (ν), and Fluorescence Quantum Yields (Φ) of NHPI, 3HNHPI, and DHNHPI (5×10^{-5} M) in $CHCl_3$.

Imide compound	λ_{abs} (nm)	ε (cm^{-1} M^{-1})	λ_{ex} (nm)	λ_{em} (nm)	ν (cm^{-1})[a]	Φ
NHPI	294	1,947	295	411	9,567[b]	0.007
3HNHPI	328	3,661	332	534	11,394	0.352
DHNHPI	372	5,091	369	427	3,681	0.507

[a] $\nu = 10^7 (1/\lambda_{ex} - 1/\lambda_{em})$.

[b] For NHPI, λ_{abs} and λ_{ex} do not correspond to $S_0 \rightarrow S_1$, but rather to $S_0 \rightarrow S_4$ transition wavelength.

To investigate why DHNHPI does not cause ESIPT emission, an imide compound having two methoxy (–OCH_3) groups (DMNHPI), instead of –OH groups, was newly synthesized. This compound should not cause an ESIPT due to a lack of *intra*-HBs. The UV-vis and fluorescent emission spectra of DHNHPI and DMNHPI dissolved in

Journal Name

ARTICLE

Table 2. Calculated Electronic Transitions of NHPI, 3HNHPI, and DHNHPI in Optimized S_0 Geometry.

Imide compound	State	Transition wavelength / nm	Oscillator strength	Orbitals			Assignment
NHPI	S_1	323.7	0.0001	HOMO–1	→	LUMO	n–π^*
	S_2	305.1	0.0005	HOMO	→	LUMO	π–π^*
	S_3	288.9	0.0000	HOMO–4	→	LUMO	n–π^*
	S_4	271.6	0.0342	HOMO–2	→	LUMO	π–π^*
	S_5	239.1	0.0956	HOMO–3	→	LUMO	π–π^*
3HNHPI *enol*	S_1	324.3	0.0930	HOMO	→	LUMO	π–π^*
	S_2	320.4	0.0001	HOMO–2	→	LUMO	n–π^*
	S_3	303.9	0.0241	HOMO–1	→	LUMO	π–π^*
	S_4	279.5	0.0000	HOMO–4	→	LUMO	n–π^*
	S_5	241.9	0.0546	HOMO–3	→	LUMO	π–π^*
3HNHPI *keto*	S_1	447.3	0.1438	HOMO	→	LUMO	π–π^*
DHNHPI *enol*	S_1	363.7	0.1498	HOMO	→	LUMO	π–π^*
	S_2	311.1	0.0001	HOMO–2	→	LUMO	n–π^*
	S_3	310.3	0.0005	HOMO–1	→	LUMO	π–π^*
	S_4	277.5	0.0000	HOMO–4	→	LUMO	n–π^*
	S_5	245.5	0.0188	HOMO	→	LUMO+1	π–π^*

$CHCl_3$ (5×10^{-5} M) are shown in Fig. S2 in the Supplementary Information. DMNHPI shows absorption (λ_{abs} = 373 nm) and emission (λ_{em} = 424 nm) peaks, of which the peak positions are almost the same as those of DHNHPI, which strongly supports the absence of ESIPTs for DHNHPI in $CHCl_3$. This prohibition of ESIPTs could be attributed to the resonance effect of the electron donating two –OH groups attached to the same phthalimide moiety. Park et al.[53,54] reported that diethylamino-substituted-2-(2'-hydroxyphenyl)benzoxazole (Et_2N-HBO) only exhibited fluorescence from the enol form without undergoing an ESIPT, despite the fact that the unsubstituted HBO is an ESIPT compound. This behavior is due to the weakening of the acidity of the –OH group induced by the high electron-donating $–Et_2N$ group. As a consequence, the ESIPT of DHNHPI is prohibited by the electron-donating –OH groups located at the *para*-position.

Fluorescence Properties under Alkaline Conditions

Under alkaline (basic) conditions, one or both of the phenolic –OH groups in DHNHPI could be deprotonated, which could cause significant changes in its fluorescence properties.[55] In this study, DBU was used as an additive reagent for $CHCl_3$ to modify the basicity of solutions. Fig. 5a and 5b show the UV-vis and fluorescent emission spectra of DHNHPI dissolved in $CHCl_3$ and mixed solutions of $CHCl_3$/DBU (5×10^{-5} M, [DBU] = 0–10^{-2} M). The calculated one-electron transitions for the mono-anion form of DHNHPI ($DHNHPI^-$) in the S_0 geometry, as well as the spatial distributions of the HOMO and LUMO, are shown in Fig. S3 in the Supplementary Information. When [DBU] is higher than 10^{-4} M, a new absorption band is observed around 440 nm, and its intensity increases with increasing [DBU] (Fig. 5a). According to the TD-DFT calculations, $DHNHPI^-$ should show an allowed $S_0 \rightarrow S_1$ transition attributable to LE(π–π^*) at 469.5 nm (Fig. S3). Thus, the experimental absorption band observed around 440 nm is assignable to the LE(π–π^*) transition of $DHNHPI^-$ generated by deprotonation of the phenolic –OH group. In the emission spectra excited at 372 nm, the fluorescence peak gradually shifts to longer wavelengths as DBU is added, compared with the neutral condition, which should be caused by the change in the polarity of the solvent. When [DBU] is higher than 10^{-4} M, a new fluorescence peak is observed at 522 nm by excitation at 449 nm, which is attributable to $DHNHPI^-$ due to the same behavior as that which causes the newly shown absorption peak. The Φ value of this emission (Φ = 0.640) is significantly higher than that observed in the neutral $CHCl_3$ (Φ = 0.507), which is explainable by the larger f value (f = 0.1525) of the $S_0 \rightarrow S_1$ transition of $DHNHPI^-$ as compared to that of the neutral enol form (f = 0.1498). When [DBU] was

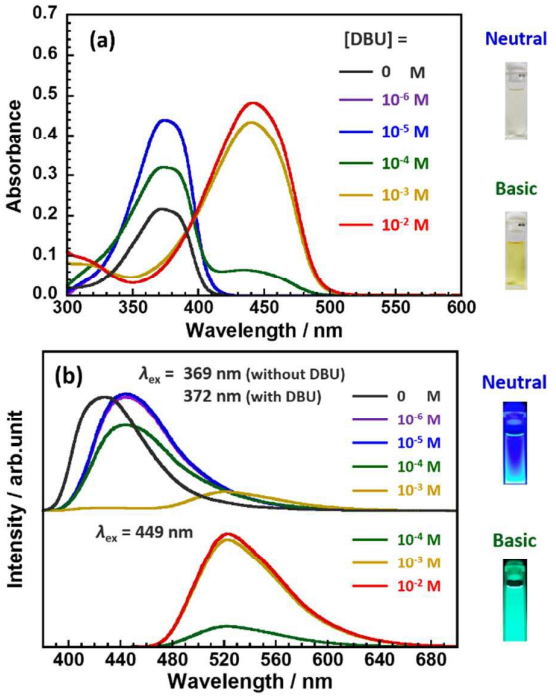

Fig. 5. (a) UV-vis and (b) emission spectra of DHNHPI (5×10^{-5} M) under neutral and alkaline conditions using $CHCl_3$/DBU mixed solutions. Excitation wavelengths are 369 nm ([DBU] = 0 M), 372 nm, and 449 nm ([DBU] = 10^{-6}–10^{-2} M), respectively.

increased beyond 10^{-2} M, the imide compound was gradually decomposed by hydrolysis, so no fluorescence peak corresponding to the dianion form ($DHNHPI^{2-}$) is observed.

Fluorescence Properties in the Solid State

Fig. 6 shows a comparison of the fluorescent emission spectra of 3HNHPI and DHNHPI in the solid (powdery) state, and in $CHCl_3$. 3HNHPI shows a broad fluorescence peak at 536 nm in the solid state, when excited at 340 nm, for which the spectrum is very similar to that observed for $CHCl_3$. This similarity indicates that 3HNHPI undergoes an ESIPT in the solid state as well as in solution. In contrast, DHNHPI shows a fluorescence peak at 447 nm with a relatively narrow width in the solid state when excited at 370 nm, which is evidently shifted to a longer wavelength by 20 nm compared with in $CHCl_3$. In addition, a weak fluorescence peak is observed at 524 nm for DHNHPI, as indicated by the arrow in Fig. 6. Intermolecular distances between imide molecules in the solid state or in concentrated solutions should be much shorter than those in diluted solutions, which can lead to the formation of dimers in the ground- or excited-states due to strong intermolecular interactions.[56,57] To illuminate the optical properties in the solid state, XRD analyses are helpful because one can obtain information not only about the structural data of one molecule, but also about the intermolecular distances and angles between adjacent molecules.[58-62] Fig. 7 shows the crystal structures of (a) 3HNHPI and (b) DHNHPI, for which the crystal data and experimental details are shown in Tables S2 and S3 in the Supplementary Information. Bilton et al.[62,63] reported that the most probable *intra*-HB motifs are

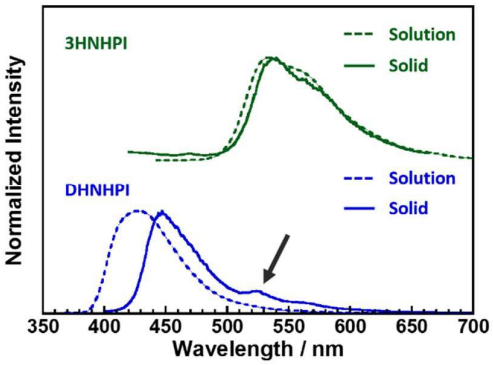

Fig. 6. Emission spectra of 3HNHPI and DHNHPI in $CHCl_3$ (broken line) and solid states (solid line). Excitation wavelengths are 332 nm (3HNHPI) and 369 nm (DHNHPI) for solution states and 340 nm (3HNHPI) and 367 nm (DHNHPI) for solid states.

planar conjugated six-membered rings with propensities for resonance-assisted HB (RAHB), in which the shortest contacts are formed between HB-donors and HB-acceptors. Both 3HNHPI and DHNHPI form RAHB structures in which π-electrons alleviate the bias of resonance charges. These can be confirmed by the fact that the distances of H1–O6 [2.354(3) Å] and O2–O6 [3.039(4) Å], and the angle of O2–H1–O6 [139.0(2)°] for 3HNHPI; and of H1A–O6 (or H1B–O9) [2.17(4) Å (or 2.64(3) Å)] and O2A–O6 (or O2B–O9) [2.938(2) Å (or 3.245(2) Å)], and the angles of O2A–H1A–O6 [140(3)°] and O2B–H1B–O9 [127(3)°] for DHNHPI, respectively, are typical values for H and O atoms which form stable *intra*-HBs (see Fig. 7 and Table S3). As shown in Fig. 7, in the molecular arrangement along the stack direction for 3HNHPI and DHNHPI, molecules are packed in a parallel but staggered style. Garry et al.[64] reported that 1,3-dichloronaphthalene (DCN) exhibits an excimer fluorescence at 398 nm with a large bathochromic shift in the solid state at 77 K. In the crystal structure of DCN, two neighboring molecules are stacked with an intermolecular distance of 3.5 Å, which is suitable for forming excimers. For DHNHPI, quasi six-membered planar rings stabilized by *intra*-HBs are stacked with adjacent molecules as indicated by the blue plane in Fig. 7. The distance between those planes (~3.3 Å) can effectively induce weak intermolecular π–π interactions, which promote the formation of excimers in the solid state. In contrast, there is no stacking of planar structures at nearby sites in 3HNHPI. The quasi six-membered ring in 3HNHPI is not overlapped with those of the neighboring molecules because it has only one *intra*-HB at the one side of the phthalimide moiety**.** Consequently, the fluorescence peak of DHNHPI observed at the longer wavelength in the solid state is explainable by stabilization effects, due to the possible π–π interactions in the excited state. As such, the weak fluorescence observed at around 525 nm could thus be attributed to the emission from the excimers.

3.2. Fluorescence Properties of PI-DHPA

Characterization of PI films

The ATR FT-IR spectra of PI-PA, PI-3HPA, and PI-DHPA films are shown in Fig. S4 in the Supplementary Information. The completion of thermal imidizations was confirmed by the C=O stretching (1780

Journal Name

ARTICLE

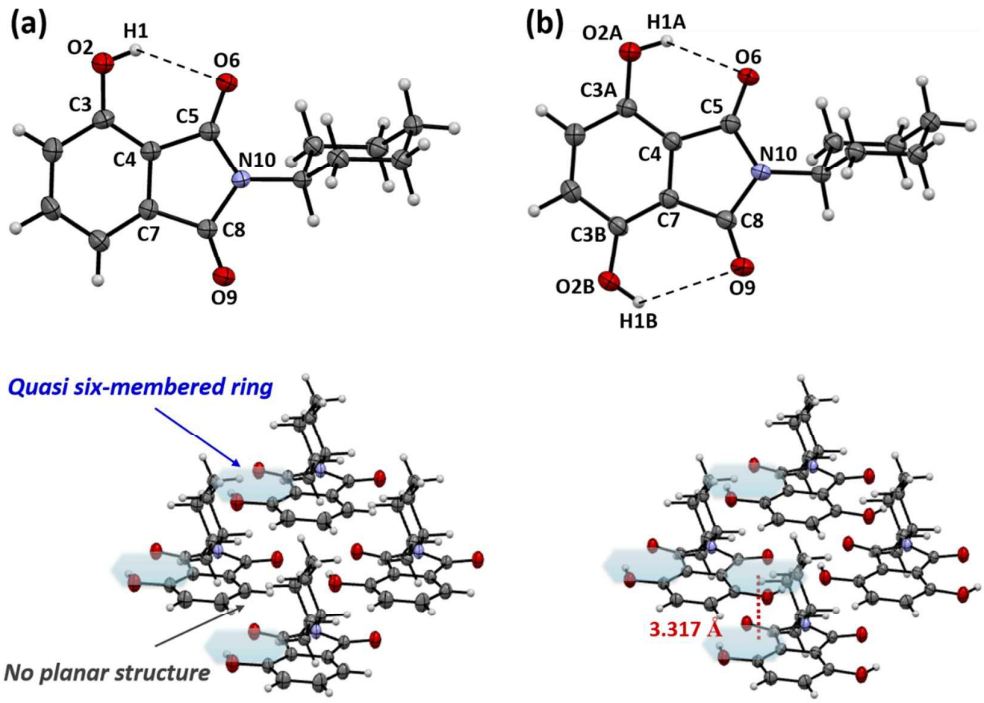

Fig. 7. Crystal structures of 3HNHPI and DHNHPI obtained from single-crystal XRD analyses.

cm^{-1}) and C–N stretching (1360 cm^{-1}) bands of the imide rings. The film thicknesses and decomposition temperatures at 5% weight loss (T_d^5) are listed in Table 3. The TGA curves of the PI films are also shown in Fig. S5 in the Supplementary Information. All of the PI films demonstrated T_d^5 values over 395 °C, due to the rigid molecular structure of the main PI chains. The excellent thermal stability is of great advantage for modern opto-electronic and photonic applications.

UV-vis Absorption and Emission Spectra

To investigate the role of the two –OH groups at the termini of the PI chain, the fluorescence properties of PI-DHPA were compared with those of PI-PA and PI-3HPA, which have unsubstituted phthalimide and 3-hydroxy-phthalimide moieties at their chain termini. Fig. 8 shows the (a) UV-vis and (b) excitation/emission spectra of the PI films; the associated λ_{ex}, λ_{em} as well as their associated Φ values measured in the solid state are listed in Table 3. Note that the UV-vis spectra of the PI films were normalized by their film thicknesses. In the UV-vis spectra of PI-PA and PI-3HPA films, only the absorption bands attributable to the LE(π–π*) bands of the ODPA-DCHM main chains were observed below 370 nm,[10,16] and no absorption bands from the end-groups were observed due to the significant overlap with those of the main chains. This can be also confirmed by the absorption spectra of NHPI and 3HNHPI in $CHCl_3$, where the absorption peaks were observed at 294 and 328 nm, respectively (see Fig. 4). In contrast, in the UV-vis spectrum of a PI-DHPA film, the LE(π–π*) band attributable to the DHPA end-groups was separately observed, in the range of 370-410 nm, from the LE(π–π*) absorption band of the main chains. As such, it is observed that the latter band is close to the absorption peak of DHNHPI in $CHCl_3$ (372 nm). When the three PIs are excited at below 350 nm, which correspond to the excitation of the main ODPA-DCHM chains, fluorescence peaks are observed at 400 nm for PI-PA and PI-3HPA and at 427 nm for PI-DHPA. When PI-DHPA is excited at 370 nm, a fluorescence peak is observed at 431 nm, which is very close to the fluorescence peak of 427 nm when excited at 332 nm. Since both the fluorescence peak positions of PI-DHPA excited at 330 nm and 370 nm differ from those of PI-PA and PI-3HPA excited at around 340 nm, the fluorescent species of the peak observed at 427–431 nm for PI-DHPA is readily attributable to the DHPA end groups (and not to the main chains). The fact that the λ_{ex} and λ_{em} of PI-DHPA are very close to those of DHNHPI dissolved in $CHCl_3$ strongly supports this view. Based on the fact that only the fluorescence from the DHPA end-groups is observed in both of the emission spectra excited at

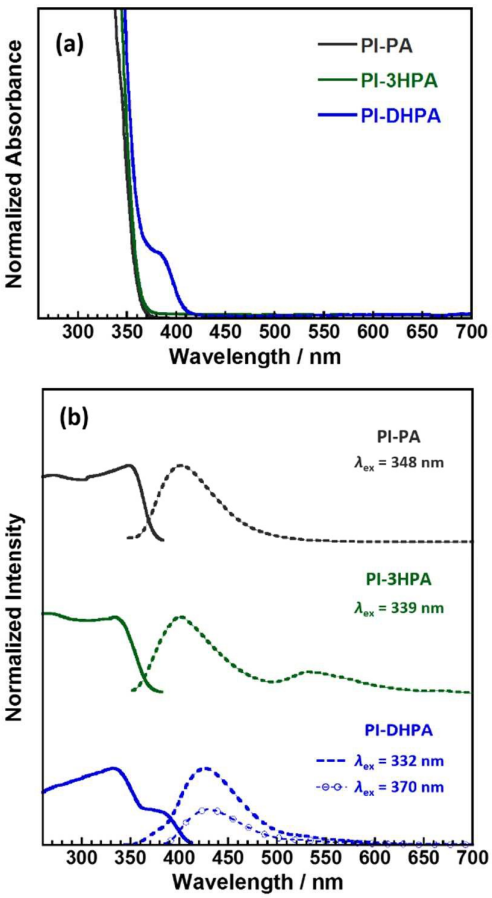

Fig. 8. (a) UV-vis spectra of PI-PA, PI-3HPA, and PI-DHPA films normalized by their film thickness and (b) excitation (solid line)/emission (broken line) spectra normalized at peak intensities. Excitation wavelengths are 348 nm for PI-PA, 339 nm for PI-3HPA, and 332 nm and 370 nm for PI-DHPA.

Table 3. Decomposition Temperatures at 5 wt% (T_d^5), Film Thicknesses, Excitation/Emission Wavelengths (λ_{ex}, λ_{em}), and Fluorescence Quantum Yields (Φ) of PI Films.

Polyimide	T_d^5 (°C)	Thickness (μm)	λ_{ex} (nm)	λ_{em} (nm)	Φ
PI-PA	395	11.9	348	402	0.076
PI-3HPA	452	22.1	339	400, 534	0.089
PI-DHPA	406	1.7	332	427	0.040
			370	431	0.059

332 nm and 370 nm, it can be concluded that highly efficient Förster resonance energy transfer (FRET) occurs from the PI main chains to the DHPA end groups upon direct excitation of the PI-DHPA main chain.[65] This behavior occurs because DHPA end groups have absorption bands in the range from 370 nm to 410 nm, which well overlaps with the fluorescent emission peak of ODPA- DCHM main chains (400 nm). A component of FRET processes (in the excited-states of PI-DHPA) is the induction of non-radiative deactivation paths, which could be a reason for the slightly lower Φ value (0.040) for PI-DHPA as compared to those of PI-PA (0.076) and PI-3HPA (0.089), because no FRET processes are induced in the latter two PIs.

Conclusions

To investigate the effects of *intra*-HBs on the fluorescence properties of imide compounds and end-capped PIs, an imide compound having two –OH groups (DHNHPI) and an end-capped PI having DHNHPI moieties at the termini (PI-DHPA) were newly synthesized, with their resulting structures and fluorescence properties extensively examined. DHNHPI demonstrated a high fluorescence quantum yield (Φ = 0.507) compared with those of NHPI and 3HNHPI in $CHCl_3$, which is supported by the large oscillator strength (f) value estimated for the $S_0 \rightarrow S_1$ transition of DHNHPI (0.1498) based on the formation of the double *intra*-HBs. However, ESIPT emission was not observed for DHNHPI due to the strong electron-donating effect of the second –OH group, resulting in an intense fluorescence peak with a relatively small Stokes shift (v = 3,463 cm^{-1}). Under non-aqueous alkaline conditions prepared by DBU, new absorption and fluorescence of the anion ($DHNHPI^-$) were clearly observed. Single-crystal XRD analysis suggested that DHNHPI induces weak intermolecular π–π interactions with neighboring molecules along the stacking direction, and thus the fluorescence peak observed around 525 nm is attributable to the excimers generated by the intermolecular interactions. In both the emission spectra of a PI-DHPA film excited at 330 nm and 370 nm, only the fluorescence peak emitted from the end groups were observed at around 430 nm, which indicates that an effective FRET was generated from the main chains to the end groups. As a consequence, the fluorescence properties of imide compounds and PIs are significantly enhanced by the introduction of two –OH groups. In particular, a judicious introduction of –OH groups, which makes imide compounds highly fluorescent and sensitive to alkaline conditions, is promising for the development of novel PIs that exhibit optical and photonic functionalities.

Acknowledgements

Single-crystal XRD data for 3HNHPI and DHNHPI were collected and analyzed by Dr. Kohei Johmoto, Ms. Aya Sakon, and Prof. Hidehiro Uekusa at Tokyo Institute of Technology. Their cooperation and efforts are greatly appreciated.

References

1 J. H. Burroughes, D. D. C. Bradley, A. R. Brown, R. N. Marks, K. Mackay, R. H. Friend, P. L. Burns, A. B. Holmes, *Nature*, 1990, **347**, 539.
2 A. C. Grimsdale, K. L. Chan, R. E. Martin, P. G. Jokisz, A. B. Holmes, *Chem. Rev.*, 2009, **109**, 897.
3 Q. Peng, Z. Y. Lu, Y. Huang, M. G. Xie, S. H. Han, J. B. Peng, Y. Cao, *Macromolecules*, 2004, **37**, 260.
4 D. Vak, J. Jo, J. Ghim, C. Chun, B. Lim, A. J. Heeger, D. Y. Kim, *Macromolecules*, 2006, **39**, 6433.

5 C. E. Sroog, *J. Polym. Sci. Macromol. Rev.*, 1976, **11**, 161.
6 M. Hasegawa, M. Kochi, I. Mita, R. Yokota, *Eur. Polym. J.*, 1989, **25**, 349.
7 Q. Li, K. Horie, R. Yokota, *J. Photopolym. Sci. Technol.*, 1997, **10**, 49.
8 S. M. Pyo, T. J. Shin, S. I. Kim, M. Ree, *Mol. Cryst. Liq. Cryst.*, 1998, **316**, 353.
9 S. Matsuda, Y. Urano, J. W. Park, C. Ha, S. Ando, *J. Photopolym. Sci. Technol.*, 2004, **17**, 241.
10 J. Wakita, H. Sekino, K. Sakai, Y. Urano, S. Ando, *J. Phys. Chem. B*, 2009, **113**, 15212.
11 J. Ishii, S. Horii, N. Sensui, M. Hasegawa, L. Vladimirov, M. Kochi, R. Yokota, *High. Perform. Polym.*, 2009, **21**, 282.
12 K. Takizawa, J. Wakita, K. Sekiguchi, S. Ando, *Macromolecules*, 2012, **45**, 4766.
13 D. Creed, C. E. Hoyle, J. W. Jordan, C. A. Pandey, R. Nagarajan, S. Pankasem, A. M. Peeler, P. Subramanian, *Macromol. Symp.*, 1997, **116**, 1.
14 M. Hasegawa, K. Horie, *Prog. Polym. Sci.*, 2001, **26**, 259.
15 A. Demeter, *React. Kinet. Catal. Lett.*, 2005, **85**, 331.
16 J. Wakita, S. Inoue, N. Kawanishi, S. Ando, *Macromolecules*, 2010, **43**, 3594.
17 A. Dreuw, J. Plotner, L. Lorenz, J. Wachtveitl, J. E. Djanhan, J. Bruning, T. Metz, M. Bolte, M. U. Schmidt, *Angew. Chem. Int. Ed.*, 2005, **44**, 7783.
18 J. E. Kwon, S. Y. Park, *Adv. Mater.*, 2011, **23**, 3615.
19 B. M. Uzhinov, M. N. Khimich, *Russ. Chem. Rev.*, 2011, **80**, 553.
20 J. Zhao, S. Ji, Y. Chen, H. Guo, P. Yang, *Phys. Chem. Chem. Phys.*, 2012, **14**, 8803.
21 D. K. Rana, S. Dhar, A. Sarkar, S. C. Bhattacharya, *J. Phys. Chem. A*, 2011, **115**, 9169.
22 Y. Su, S. Chai, *J. Photochem. Photobiol. A: Chem.*, 2014, **290**, 109.
23 V. Enchev, N. Markova, M. Stoyanova, P. Petrov, M. Rogozherov, N. Kuchukova, I. Timtcheva, V. Monev, S. Angelova, M. Spassova, *Chem. Phys. Lett.*, 2013, **563**, 43.
24 H. Zhang, P. van der Meulen, M. Glasbeek, *Chem. Phys. Lett.*, 1996, **253**, 97.
25 D. Marks, P. Prosposito, H. Zhang, M. Glasbeek, *Chem. Phys. Lett.*, 1998, **289**, 535.
26 P. Prosposito, D. Marks, H. Zhang, M. Glasbeek, *J. Phys. Chem. A*, 1998, **102**, 8894.
27 P. Toele, H. Zhang, M. Glasbeek, *J. Phys. Chem. A*, 2002, **106**, 3651.
28 P. Toele, M. Glasbeek, *Chem. Phys, Lett.*, 2005, **407**, 487.
29 D. A. Yushchenko, V. V. Shvadchak, M. D. Bilokin, A. S. Klymchenko, G. Duportail, Y. M'ely, V. G. Pivovarenkoa, *Photochem. Photobiol. Sci.*, 2006, **5**, 1038.
30 S. R. Va'zquez, M. C. R. Rodriguez, M. Mosquera, F. R. Prieto, *J. Phys. Chem. A*, 2007, **111**, 1814.
31 D. McMorrow, M. Kasha, *J. Am. Chem. Soc.*, 1983, **105**, 5133.
32 A. J. G. Strandjord, P. F. Barbara, *J. Phys. Chem.*, 1985, **89**, 2355.
33 M. Kasha, *J. Chem. Soc., Faraday Trans. 2*, 1986, **82**, 2379.
34 O. K. Abou-Zied, R. Jimenez, E. H. Z. Thompson, D. P. Millar, F. E. Romesberg, *J. Phys. Chem. A*, 2002, **106**, 3665.
35 J. Seo, S. Kim, S. Y. Park, *J. Am. Chem. Soc.*, 2004, **126**, 11154.
36 P. K. Sengupta, M. Kasha, *Chem. Phys. Lett.*, 1979, **68**, 382.
37 A. Fin, I. Petkova, D. A. Doval, N. Sakai, E. Vauthey, S. Matile, *Org. Biomol. Chem.*, 2011, **9**, 8246.
38 M. F. Ansell, B. W. Nash, D. A. Wilson, *J. Chem. Soc.*, 1963, 3028.
39 T. R. Kelly, S. H. Bell, N. Ohashi, *J. Am. Chem. Soc.*, 1988, **110**, 6471.
40 R. Le Vezouet, A. J. P. White, J. N. Burrows, A. G. M. Barrett, *Tetrahedron*, 2006, **62**, 12252.
41 J. F. Tannaci, M. Noji, J. McBee, T. D. Tilley, *J. Org. Chem.*, 2007, **72**, 5567.
42 N. Savjani, S. J. Lancaster, S. Bew, D. L. Hughes, M. Bochmann, *Dalton Trans.*, 2011, **40**, 1079.
43 Y. Oishi, K. Ogasawara, H. Hirahara, K. Mori, *J. Photopolym. Sci. Technol.*, 2001, **14**, 37.
44 Y. Oishi, N. Kikuchi, K. Mori, S. Ando, K. Maeda, *J. Photopolym. Sci. Technol.*, 2002, **15**, 213.
45 G. M. A. Sheldrick, *Acta Cryst.*, 2008, **A64**, 112.
46 C. Lee, W. Yang, R. G. Parr, *Phys. Rev.*, 1988, **B37**, 785.
47 B. Miehlich, A. Savin, H. Stoll, H. Preuss, *Chem. Phys. Lett.*, 1989, **157**, 200.
48 A. D. Cecke, *J. Chem. Phys.*, 1993, **98**, 5648.
49 M. J. Frisch, et al., GAUSSIAN 09 (Revision B.01), Gaussian Inc., Wallingford, CT, 2010.
50 G. A. Jeffrey, *An Introduction to Hydrogen Bonding*, Oxford University Press, Springer, Oxford, 1997.
51 T. Steiner, *Angew. Chem. Int. Ed.*, 2002, **41**, 48.
52 H. Houjou, T. Motoyama, S. Banno, I. Yoshikawa, K. Araki, *J. Org. Chem.*, 2009, **74**, 520.
53 J. Seo, S. Kim, S. Park, S. Y. Park, *Bull. Korean Chem. Soc.*, 2005, **26**, 1706.
54 S. Park, S. Kim, J. Seo, S. Y. Park, *Macromolecules*, 2005, **38**, 4557.
55 M. Zahid, G. Grampp, A. Mansha, I. A. Bhatti, S. Asim, *J. Fluoresc.*, 2013, **23**, 829.
56 M. V. Auweraer, A. Gilbert, F. C. Schryver, *J. Am. Chem. Soc.*, 1980, **102**, 4007.
57 N. Kizu, M. Itoh, *J. Am. Chem. Soc.*, 1993, **115**, 4799.
58 J. L. Scott, T. Yamada, K. Tanaka, *Bull. Chem. Soc. Jpn.*, 2004, **77**, 1697.
59 A. Szemik-Hojniak, I. Deperasinska, L. Jerzykiewicz, P. Sobota, M. Hojniak, A. Puszko, N. Haraszkiewicz, G. van der Zwan, P. Jacques, *J. Phys. Chem. A*, 2006, **110**, 10690.
60 C. Kitamura, C. Matsumoto, N. Kawatsuki, A. Yoneda, K. Asada, T. Koboyashi, H. Naito, *Bull. Chem. Soc. Jpn.*, 2008, **81**, 754.
61 T. Hinoue, Y. Shigenoi, M. Sugino, Y. Mizobe, I. Hisaki, M. Miyata, N. Tohnai, *Chem. Eur. J.*, 2012, **18**, 4634.
62 C. Bilton, F. H. Allen, G. P. Shields, J. A. K. Howard, *Acta Cryst.*, 2000, **B56**, 849.
63 G. Gilli, F. Bellucci, V. Ferretti, V. Bertolasi, *J. Am. Chem. Soc.*, 1989, **111**, 1023.
64 G. E. Berkovic, Z. Ludmer, *J. Lumin.*, 1982, **26**, 463.
65 N. J. Turro, V. Ramamurthy, J. C. Scaiano, *Modern Molecular Photochemistry of Organic Molecules*, University Science Books, Sausalito, California, 2009.